1 nternational Geoscience and Remote Sensing Symposium, 1996

K_u-Band Ocean Backscatter Functions for Surface Wind Retrieval

S. V. Nghiem, l?. K. Li, and G. Neumann
Jet l'repulsion Laboratory
California Institute of Technology
Pasadena, California

Mailing address: Dr. S. V. Nghiem, Jet Propulsion Laboratory
Mail Stop 300-235, 4800 Oak Grove Drive, Pasadena, CA 91109

K_u-Band Ocean Backscatter Functions for Surface Wind Retrieval

S. V. Nghiem, F. K. Li, and G. Neumann

Jet Propulsion Laboratory, MS 300-235
California Institute of Technology
4800 Oak Grove Drive, Pasadena, CA 91109, USA
Tel: 818-354-2982, Fax: 818-393-5285
E-mail: nghiem@malibu.jpl.nasa.gov

Abstract The accuracy of wind measurements with scatterometer techniques depends on the particular geophysical model function used in the retrieval algorithm. Discrepancies among existing model functions, developed based on a mixture of aircraft and satellite backscatter data acquired two decades ago, will result in differences in retrieved wind fields. The Jet Propulsion Laboratory airborne Ku-band NUSCAT scatterometer was used to obtain au extensive data set over a wide range of wiud conditions to provide a more accurate. study of ocean radar backscatter signatures. Backscatter were measured during the Surface Wave Dynamics Experiment in au oceanic area off the US East coast. Backscatter data were obtained for both horizontal aud vertical polarizations, incidence angle from 10° to 60°, aud wiud speeds up to 15 $m \cdot s^{-1}$. The measured results arc compared with calculated values to assess the existing geophysical model functions for applications to ocean surface wind retrieval.

INTRODUCTION

K_u- band scatterometer technology has been demonstrated and will be used to monitor global ocean wiud fields from spat.eborllc sensors such as the NASA Scatterometer (NSCAT) [I]. Algorithms for retrieval of wind speeds and directions from scatterometer data utilize absolute radar returns as well as relative azimuth modulations of backscatter [3]. The accuracy of the wind retrieval depends on the particular geophysical model function used in the algorithm.

Among the existing geophysical model functions arc RADSCAT [2], SASS-1 [3], aud SASS-II [4, 5] developed based on aircraft and satellite backscatter data acquired in the 1970s. With advances in both scatterometer and buoy technologies, au extensive data set over a wide range of wind conditions will allow a more accurate assessment of the ocean radar backscatter.

In this paper, Ku-baud backscatter functions of neutral wind arc studied based on the NUSCAT-SWADE data base. NUSCAT is au airborne K_u-band scatterometer developed by the Jet Propulsion Laboratory. NUSCAT was used to measure ocean backscatter during the Surface Wave Dynamics Experiment (SWADE). Ten flights resulted in 30 hours of data collection were conducted on the NASA Ames C130 aircraft during SWADE in February and March of 1991 off the coast of Maryland and Virginia over several ocean buoys. NUSCAT data together with buoy wiud speeds and directions arc used in this analysis.

AZIMUTH MODULATIONS

A second harmonic function has been adopted to describe ocean aziumth modulation in radar backscatter σ^0 [2, 3, 4, 6]. This function is determined by three different coefficients /Jo, Al, aud A_2 as follows

$$\sigma^0(U,\chi,\theta,P) = A_0(U,\theta,P) + A_1(U,\theta,P)\cos(\chi) + A_2(U,\theta,P)\cos(2\chi)$$

where A_0 is the mean backscatter, A_1 is for the upwind and downwind asymmetry, and A_2 is for the difference in backscatter extrema. Each of these coefficients depends on wiud speed U, incidence angle θ, aud polarization P (HH or VV). Angle χ is the azimuth defined with respect to upwind where $\chi = 0$. In the geophysical model functions, wind speed U is the neutral wind speed U_N(19.5 m) at the height of 19.5 m above sea surface level [2, 3, 4, 5].

During the NUSCAT flights ou the C130, a difference between operational aud desired pitch angles of the aircraft caused a tilt of the antenna axis with respect to the nominal incident angle. As a result, the incidence angle was modulated as the antenna scanned through the 360° azimuth. Extraneous harmonics were thereby created in the measu red signals by the beating between the incidence angle modulations and the physical ocean backscatter modulations. To account for this effect, a harmonic analysis method independent of a priori geophysical model functions is developed, tested, aud implemented. This method also fiuds the upwind backscatter maximum without relying on buoy data for wind direction measurements. In this method, there arc two problems need to be considered. First, there exist different solutions for wind directions at azimuth angles with 180° apart. This causes a confusion between upwind and downwind directions. To resolve this problem, we usc buoy data for wiud directions which need to be known only to within ±90° for this purpose. The second problem occurs when the wind direction is parallel to the azimuth direction where the incidence modulation is au extremum. In this situation, the information carried in the backscatter data alone is not adequate to separate the contributions by the ocean modulations and by the incidence modulations to the total first harmonic term. In these cases, significant errors arc incurred when the variations in the incidence angle arc very close to the sinusoidal form. To avoid the errors, we exclude cases where retrieved wind angles are close to the extremum azimuth angles of the incidence modulation.

OCEAN BACKSCATTER

We apply the above method to the NUSCAT backscatter data to determine azimuth modulations in ocean backscatter over the wind conditions encountered during SWA 1)E. For the results below, w c exclude cases with large swells and sea sur-face temperature differences across the Gulf Stream boundary to avoid complicated air and sea conditions. Buoy measurements at the closest time and locat ion to N USCAT arc selected to correlate with the backscatter data. We will present the results in terms of upwind, downwind, aud crosswind backscattering coefficients (σ_u^0, σ_d^0, and σ_c^0, respectively), which determine the coefficients A_0, A_1 , aud A_2 in the backscatter harmonic function with the following relations

$$A_0 = \frac{1}{4}(\sigma_u^0 + \sigma_d^0 + 2\sigma_c^0)$$

$$A_1 = \frac{1}{2}(\sigma_u^0 - \sigma_d^0)$$

$$A_2 = \frac{1}{4}(\sigma_u^0 + \sigma_d^0 - 2\sigma_c^0)$$

To check the data processing, wc examine the result of a case obtained during 11'li.gilt 1 on 27 February 1991 over buoy 44015 (Discus E), where NUSCAT was less than 10 km from the buoy aud within 2.4 minutes from buoy wind measurements and 13.6 minutes from buoy wave data acquisition. The wind direction obtained by NUSCAT is at 289°, which is very c. 1osc to the wind direction at 294° measured by Discus E. In this case, the wind direction is almost parallel to the principal wave direction at spectral peak, which is at 292°. The corresponding directional wave spectrum measured by the buoy Snows that most of the wave components propagate in the same direction of the wind. The wind speed from buoy is 9.8 m s^{-1} at 4-m height, which corresponds to a neutral wiud of 11.7 111. s^{-1} at 19.5 m. Backscatter for this case compares well with SASS-11 values.

Fig. 1 presents upwind backscatter at incidence angles from 0° to 60° for the horizontal polarization. The range of wind speeds is from 4 m . s^{-1} to 15 m . s^{-1}. NUSCAT-SWA DE results represented by symbols for different incidence angles arc compared with RADSCAT results (continuous curves) aud calculated valued from SASS-I (dashed curves) and SASS-II (dashed-dotted curves). Discrepancies among the RADSCAT, SASS-f, aud SASS-11 are seen in Fig. 1. Empirical functions obtained from NUSCAT data arc also plotted with the dotted curves. In general, NUSCAT 1111 data arc higher than RADSCAT results. R ADSCAT values arc the lowest compared to SASS-1 and II. overall, NUSCAT HH backscatter compares best with the SASS-II results as seen in Figure 1. At 10° incidence angle, NUSCAT backscatter is closest to SASS-1; however, the results arc insensitive to the wiud speed and arc quite comparable to each other. NUSCAT, SASS-1, and SASS-11 are in good agreement while RADSCAT is low for incidence angles at 20° aud 30°. For 400 NUSCAT fits well with SASS-II at, wind speeds higher than 10 m s^{-1} , where mauy NUSCAT data arc located, while RADSCAT and SASS-1 arc low. For backscatter cross sections at 50°, NUSCAT, RADSCAT, and SASS-II arc in good agreement while SASS-J is low. At 60°, NUSCAT compares well with SASS-J] for wind larger than 10 111. s^{-1} while RADSCAT is significantly lower. Backscatter results for downwind and crosswind directions arc plotted in Figs. 2 and 3, where similar results arc observed. Note that at 50°, NUSCAT agrees with SASS-11, which is higher than both SASS-1 aud RADSCAT. The analysis presented in this paper is also applied to ocean backscatter with the vertical polarization.

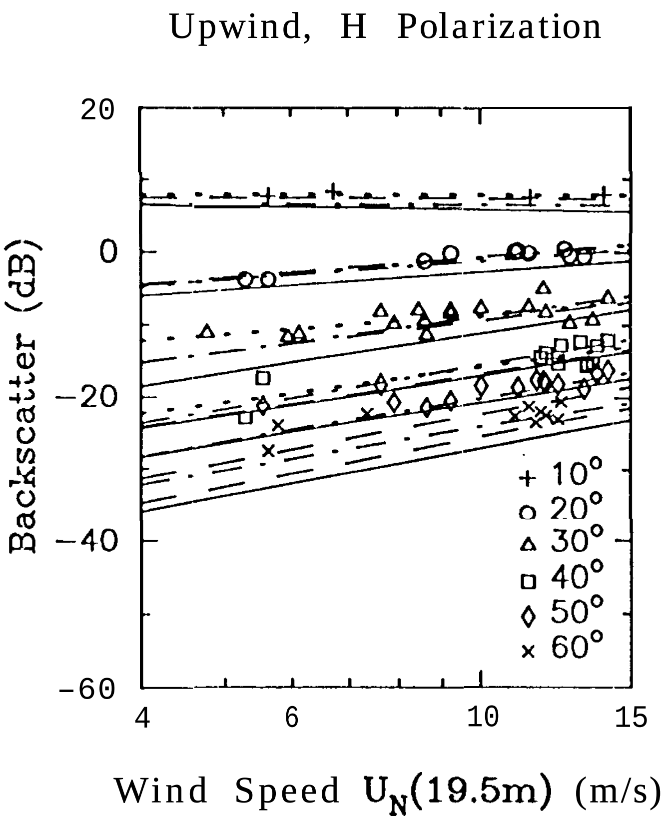

Figure 1. Upwind horizontal backscatter functions of neutral wind speed at 19.5 m. ***Symbols*** arc for NUSCAT backscatter data, dotted curves for NUSCAT fits, continuous curves for RADSCAT, dashed curves for SASS-I, and dashed-dotted curves for SASS-II,

SUMMARY

Ocean backscatter at K_u band was successfully measured by the Jet Propulsion laboratory NUSCAT scatterometer during SWADE over a wide range of wind speeds. NUSCAT results for ocean backscatter in terms of upwind, downwind, aud crosswind radar ret urns arc com-

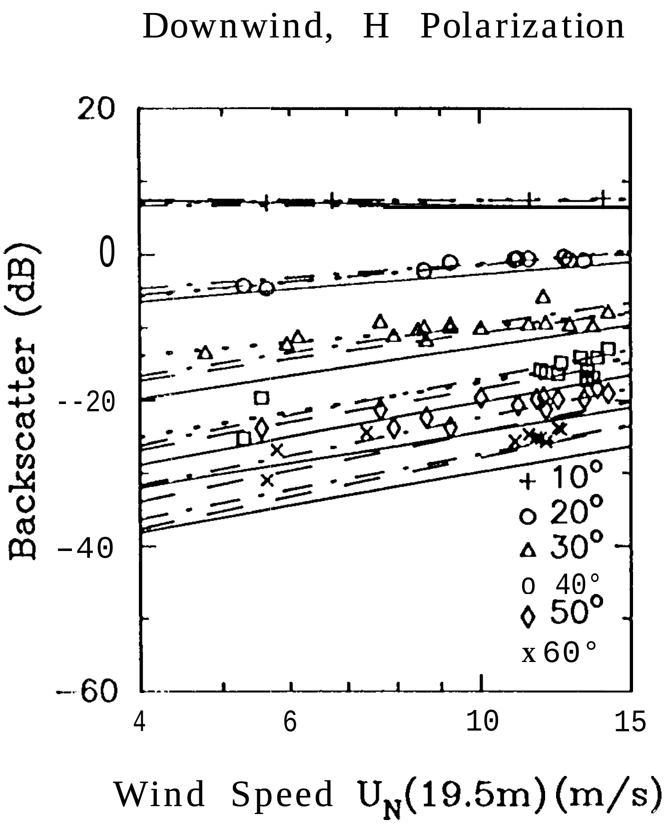

Figure 2. Downwind horizontal backscatter functions of neutral wind speed at 19.5 m. Symbols are for NUSCAT backscatter data, dotted curves for NUSCAT fits, contiguous curves for RADSCAT, dashed curves for SASS-I, and dashed-dotted curves for SASS-II.

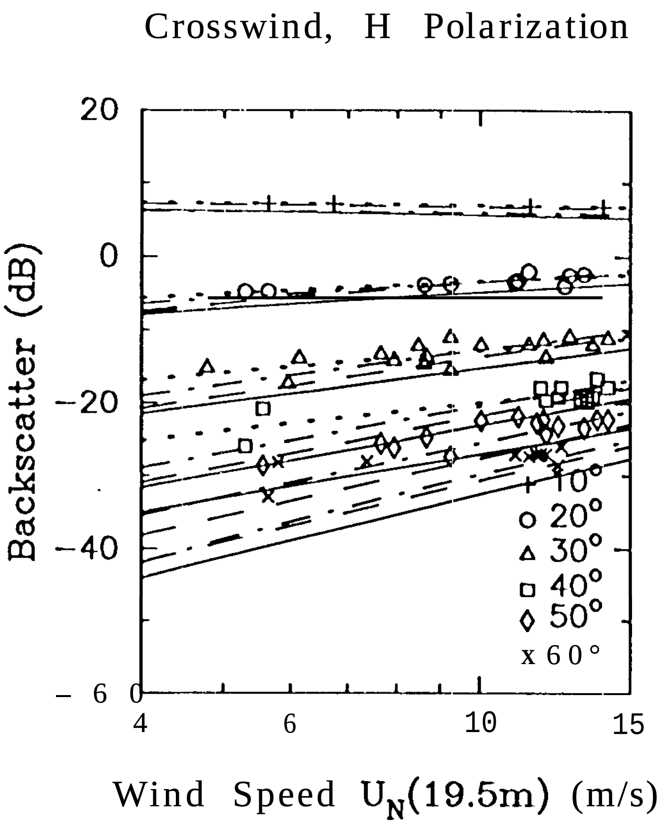

Figure 3. Crosswind horizontal backscatter functions of neutral wind speed at 19.5 m. Symbols are for NUSCAT backscatter data, dotted curves for NUSCAT fits, continuous curves for RADSCAT, dashed curves for SASS-I, and dashed-dotted curves for SASS-II.

pared to airborne RADSCAT results and to SASS-I and II geophysical model functions versus neutral wind speed. NUSCAT backscatter is closest overall to SASS-II values, fit best with SASS-I at 10° incidence angle, and are significantly higher than RADSCAT. Empirical relations between backscatter and neutral wind speed are derived for 10° to 40° incidence angles. An error analysis of the derived relations show an overall deviation factor in the order of 1 dB for ocean signatures including uncertainties in surface conditions.

ACKNOWLEDGMENTS

This work was performed under a contract with the National Aeronautics and Space Administration at the Jet Propulsion Laboratory, California Institute of Technology. The authors thank Dr. J. D. Oberholtzer, Dr. K. Steele, and Dr. D. Wang for the buoy data.

REFERENCES

[1] F. M. Naderi, M. H. Freilich, and D. G. Long, "Spaceborne radar measurement of wind velocity over the ocean an overview of the NSCAT scatterometer system," *Proceedings of the IEEE*, vol. 79, no. 6, pp. 850-866, 1991.

[2] L. C. Schroeder, D. H. Boggs, G. Dome, I. M. Halberstam, W. L. Jones, W. J. Pierson, and F. J. Wentz, "The relationship between wind vector and normalized radar cross section used to derive SEASAT-A satellite scatterometer winds," *J. Geophys. Res.*, vol. 87, no. C5, pp. 3318-3336, 1982.

[3] L. C. Schroeder, P. R. Schaffner, J. L. Mitchell, and W. L. Jones, "AAFE RADSCAT 13.9-GHz measurements and analysis: Wind-speed signature of the ocean," *IEEE J. Oceanic Engineering*, vol. OE-10, no. 4, pp. 346-357, 1985.

[4] F. J. Wentz, S. Peteherych, and L. A. Thomas, "A model function for ocean radar cross sections at 14.6 GHz," *J. Geophys. Res.*, vol. 89, no. C3, pp. 3689-3704, 1984.

[5] F. J. Wentz, L. A. Mattox, and S. Peteherych, "New algorithms for microwave measurements of ocean winds: Applications to SEASAT and the Special Sensor Microwave Imager," *J. Geophys. Res.*, vol. 91, no. C2, pp. 2289-2307, 1986.

[6] F. K. Li, G. Neumann, S. Shaffer, and S. L. Durden, "Studies of the location of azimuth modulation minimum for Ku band ocean radar backscatter," *J. Geophys. Res.*, vol. 93, no. C7, pp. 8229-8238, 1988.